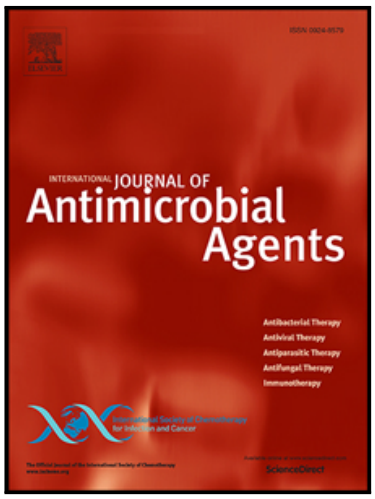


# Antimicrobial efficacy and mechanism of action of poly(amidoamine) (PAMAM) dendrimers against opportunistic pathogens.

Amy M. Holmes , Jon R. Heylings , Ka-Wai Wan , Gary P. Moss

PII: S0924-8579(18)30382-0
DOI: https://doi.org/10.1016/j.ijantimicag.2018.12.012
Reference: ANTAGE 5620

To appear in: *International Journal of Antimicrobial Agents*

Received date: 24 May 2018
Accepted date: 22 December 2018

Please cite this article as: Amy M. Holmes , Jon R. Heylings , Ka-Wai Wan , Gary P. Moss , Antimicrobial efficacy and mechanism of action of poly(amidoamine) (PAMAM) dendrimers against opportunistic pathogens., *International Journal of Antimicrobial Agents* (2018), doi: https://doi.org/10.1016/j.ijantimicag.2018.12.012

Highlights

- The aim of this study was to investigate a range of PAMAM dendrimer generations against Gram-positive and Gram-negative skin pathogens and to determine any differences in antimicrobial potency for different generations, characterising how differences in physicochemical properties influence antimicrobial efficacy.
- The results of this study indicate that the antimicrobial efficacy of native PAMAM dendrimers is dependent on generation, concentration and terminal functionalities.
- There was a strong correlation between membrane disruption and the determined biocidal activity, making it a key contributing mechanism of action.
- Selection of the type of PAMAM dendrimer is important as their inherent antimicrobial efficacy varies according to their individual physicochemical properties.

# Antimicrobial efficacy and mechanism of action of poly(amidoamine) (PAMAM) dendrimers against opportunistic pathogens.

**Amy M. Holmes[2], Jon R. Heylings[1], Ka-Wai Wan[3] & Gary P. Moss***

School of Pharmacy, Keele University, Keele, Staffordshire ST5 5BG, UK (g.p.j.moss@keele.ac.uk)

[1]Dermal Technology Laboratory Ltd., MedIC4, Keele University Science and Innovation Park, Keele, Staffordshire, ST5 5NL, UK

[2]Current address: School of Pharmacy and Medical Sciences, University of South Australia, Adelaide, South Australia, 5000 (amy.holmes@unisa.edu.au).

[3]Current address: School of Pharmacy and Biomedical Sciences, University of Central Lancashire, Preston, UK

*For correspondence:

Gary P. Moss

School of Pharmacy

Keele University

Keele

Staffordshire, ST5 5BG, UK

Email: g.p.j.moss@keele.ac.uk

Tel: +44(0)1782734776

**ABSTRACT**

The aim of this study was to investigate a range of poly(amidoamine) (PAMAM) dendrimer generations against Gram-positive and Gram-negative skin pathogens and to determine any differences in antimicrobial potency for different generations, characterising how differences in physicochemical properties influence antimicrobial efficacy. A range of tests were carried out, including viable count assays to determine $IC_{50}$ values for each dendrimer, membrane integrity studies and an inner membrane permeabilisation assay. This is supported by scanning electron microscopy imaging of the interactions observed between dendrimers and bacteria. The results of this study indicate that the antimicrobial efficacy of native PAMAM dendrimers is dependent on generation, concentration and terminal functionalities, for example the $MIC_{50}$ (υg/mL) against S. aureus was between 26.77 for the G2-PAMAM-$NH_2$ dendrimer and 2.881 for the G5-PAMAM-$NH_2$ dendrimer. There was a strong correlation between membrane disruption and the determined biocidal activity, making it a key contributing mechanism of action. This study demonstrates that selection of the type of PAMAM dendrimer is important as their inherent antimicrobial efficacy varies according to their individual physicochemical properties. This understanding may pave the way for the development of enhanced dendrimer-based antimicrobial formulations and drug delivery systems.

**Key words:** Polyamidoamine dendrimers; Skin; Biocide; Novel antiseptic; Antimicrobial

## 1. Introduction

The skin is normally colonised by a diverse range of commensal microorganisms; when a patient's immune system is compromised or the skin barrier is impaired these microorganisms may then elicit an infection. Many such infections arise from the patient's own microbial flora, with the most prominent pathogen being *Staphylococcus aureus*. *S. aureus* typically resides within the anterior nares and perineum[1] and those patients colonised on hospital admission are at a greater risk of developing surgical-site incision infections. It has also been shown to spread epidemically between patients and can be transferred from staff to patients, and vice versa[2].

Strategies in synthetic chemistry aimed at developing improved antimicrobials have traditionally focused on identifying orally bioavailable small drug molecules, often utilising high-throughput screening methods[3], an approach that has not yet translated into the availability of novel antibiotics in the clinic, particularly in light of growing microbial resistance. Biological targets, such as bacterial cell membranes, consist of macromolecules that rely on polyvalent interactions in their binding[4]. Most biological targets are of a nano-scale (1-100 nm) and therefore polyvalent macromolecules of a similar size may have increased biological efficacy when compared to small-molecule drugs due to a match in scale and multivalent binding[3]. For example, silver nanoparticles with a 1 to 10 nm size range were shown to have a greater direct interaction with bacteria than particles >10 nm in diameter[5], and silver complexes of PAMAM dendrimers have been shown to be effective against S. *aureus*, *E. coli* and *Pseudomonas aeruginosa in vitro*[6].

Polyamidoamine (PAMAM) dendrimers have become the most widely investigated dendrimers for a range of biomedical applications[7-9]. Their highly branched and globular nature gives them unique properties which enable them to function as a multivalent biocide or a nano-scale platform for antimicrobial drug delivery[10]. The uniform branching of dendrimers provides a large surface-area-to-

volume ratio, enabling high reactivity with microorganisms *in vivo*[11]. The highly localized and dense occurrence of functional groups on the dendrimer's surface can be tailored for antimicrobial efficacy or for the conjugation of targeting ligands to a variety of a microorganism's receptors[12,13].

The antimicrobial properties of unmodified PAMAM dendrimers against ocular pathogens was explored by Calbaretta and co-workers[14]. They found that the amine terminated G5-PAMAM dendrimer was toxic to *P. aeruginosa* with an $MIC_{50}$ of 1.5 ± 0.1 µg/mL, but less so for *S. aureus* (20.8 ± 3.4 µg/mL). It was demonstrated that a partial coating of the amine groups with (PEG) reduced the toxicity of the G5-PAMAM against human corneal epithelial cells whilst retaining high toxicity against *P. aeruginosa* with a $MIC_{50}$ of 0.9 ± 0.1 µg/mL. PEGylation (polyethylene glycol) of the G5-PAMAM resulted in a further decrease in efficacy against the Gram positive *S. aureus*[14]. Further, they separately reported that, even though G5-PAMAM-$NH_2$ has a greater localization of amines at its surface compared to G3-PAMAM, the potency was not increased[15].

Thus, the aim of this study was to investigate a range of PAMAM dendrimer generations, including amine- and carboxyl-terminated dendrimers, against Gram-positive and Gram-negative skin pathogens and to determine any differences in antimicrobial potency for different generations, and thus characterise how differences in molecular weights and surface charge affects antimicrobial efficacy.

## 2. Materials and Methods

### 2.1. Microdilution broth with viable count assay to determine inhibitory concentration ($MIC_{50}$)

Bacterial culture grade petri dishes, universals and pipette tips were all purchased from Startstedt (Leicester, UK). Bacterial growth medium, Mueller-Hinton agar (MHA) and Mueller-Hinton broth (MHB) were obtained from Oxoid (Basingstoke, UK). The cation content ($Mg^{2+}$ and $Ca^{2+}$) was adjusted in line with recommendations from the Clinical and Laboratory Standards Institute (CLSI)[16]. All salts used in diluents or media were reagent grade and purchased from Fisher (Loughborough, UK). *S. aureus* (ATCC 11832) and *E. coli* (ATCC 8277) were plated out on respective cation-adjusted MHA using a streak plate method to ensure growth of single colonies. The inoculated MHA plates were inverted and incubated at 37°C ± 1°C for 18-24 hours in aerobic conditions. After incubation, 3-4 single colonies were swabbed with a sterile loop and used to inoculate 10 ml of cation adjusted MHB which was then incubated at 37°C ± 1°C for 18 hours. The dense overnight inoculum was then diluted to an absorbance of 0.140 using a UV-Vis spectrophotometer (Hitachi, U1-900, Berkshire, UK) to achieve an inoculum density of ~$10^7$ cells/mL. The bacterial cell density at an absorbance of 0.140 was confirmed by diluting the bacteria and counting the cells using a haemocytometer. The inoculum was then further diluted in cation adjusted MHB to achieve a test inoculum of $1x10^5$ cells/mL.

PAMAM dendrimers (generations G2-G5; Sigma Aldrich, Dorset, UK) at varying concentrations in methanol (MeOH) were prepared at concentrations ranging from 500-1 µg/mL in ultrapure sterile water. Each PAMAM dendrimer concentration was tested in triplicate and 50 µL of each solution was plated onto a sterile 96-well plate. 50 µL of the inoculum was added to each well, except for 3 wells with cation-adjusted MHB and sterile water only as a sterility control. A growth control was tested in parallel without the addition of PAMAM dendrimer and a positive control of gentamicin 1 mg/mL was included. The 96-well plate was then incubated at 37°C ± 1°C for 2 hours and shaken at 200 rpm.

After a two hour incubation period, each well (excluding sterility control) was serially diluted 1:10 in cation-adjusted MHB to achieve a range of dilutions down to 1:100,000 and then further agitated using a sterile pipette tip. 50 µL of each dilution was plated onto a petri dish using the pour plate method with the addition of 25 mL of molten MHA at 45°C. The plates were then inverted and incubated for 18-24 h at 37°C ± 1°C in aerobic conditions. Post incubation, bacterial colonies on each plate were manually counted using a click counter. The dilutions where 30-300 colony forming units (CFUs) had grown for each growth control or PAMAM test concentration were selected. Each test concentration was tested in triplicate and the inhibition percentage was calculated using Equation 2.1. The data was then plotted as a graph of log (inhibitor) versus normalized response to determine the $MIC_{50}$ (Equation 1) usingGraphPad Prism® version 5 (San Diego, USA).

$$Inhibition\ \ percentage\ \% = (100 - \left(\frac{treated\ count}{growth\ control\ count}\right) \times 100)$$

**Equation 1 Inhibition percentage calculation**

$$Y = \frac{100}{(1 + 10^{((LogIC50 - X) \times Hillslope)})}$$

**Equation 2 Calculation of $MIC_{50}$concentration**

The log (dose) response curve follows a sigmoidal curve and the data was normalized to the growth control as 100%. The normalized model forces the curve from 0% to 100%. This is ideal for the calculation of the $MIC_{50}$ *i.e*. the concentration at 50% growth inhibition. This model also does not assume a standard hill slope of 1.0 but fits the hill slope from the data therefore it is a variable

slope model that is ideal when there are many data points. The broth microdilution assays to calculate the $MIC_{50}$ concentrations were ran as *n*=9 therefore this model was ideal.

**2.2. Membrane integrity study**

The membrane integrity study was modified from the method outlined in Chen and Cooper.[27] *S. aureus* (ATCC 11832), *S. epidermidis* (ATCC 12228) and *E. coli* (ATCC 8277) were plated on tryptone soya agar (TSA) plates using a streak method. The inoculated plates were inverted and incubated at 37°C ± 1°C for 18-24 hours in aerobic conditions. After the incubation period 2-3 single colonies were removed using a sterile loop and used to inoculate tryptone soya broth (TSB). The inoculated TSB was then incubated for 18 h at 37°C ± 1°C. Post-incubation period the inoculated TSB was then centrifuged at 1000 x *g* for 10 mins to harvest the bacterial cells, with the resultant pellet resuspended in 1x phosphate-buffered saline (PBS, pH 7.4). This was centrifuged (as above) and the supernatant discarded. The pellet was washed and resuspended in PBS and the absorbance was adjusted to 0.7 at 420 nm to dilute the cells to a final test suspension. A 3 mL aliquot of the final bacterial inoculum was added to a 3 mL aliquot of the PAMAM dendrimer solution at a concentration of 10 x the calculated $MIC_{50}$ for each respective PAMAM dendrimer generation. At different time points (20, 40, 60, and 120 min) a 1.5 mL aliquot of the sample was removed and immediately syringe-filtered using a 0.22 µm syringe filter (Millipore MCE sterile 33 mm filter, Watford, UK). The particulate-free supernatant was analysed at 260 nm by UV spectrometry (Hitachi, U1-900, Berkshire, UK), with the absorbance being plotted against each time point.

**2.3. Inner membrane permeabilisation assay**

Inner membrane permeabilisation was determined by the release of cytoplasmic β-galactosidase from *E. coli* into the culture medium in a method modified from Je and Kim (2006)[28]. *E. coli* was cultured, harvested and washed and re-suspended in 0.5% NaCl. *E. coli* was re-suspended at an

absorbance of 0.6 at 420 nm and 100 µL of the test inoculum was transferred into each well of a 96-well plate. 100 µL of PAMAM dendrimer (generations 2, 3, 3.5, 4 and 5 at concentrations of 0.1, 1, 5, 10, 25 and 50 µg/mL was added to each well. Also, 10 µL of a 30 mM *ortho*-nitrophenyl-β-galactoside (ONPG; Sigma – Dorset, UK) solution was added to each well. A blank of *E. coli* with ONPG without PAMAM dendrimer was used as a negative control and a vehicle control was also run in parallel. The production of *O*-nitrophenol was measured every 2 minutes for 12 minutes by monitoring the absorbance at 420 nm in a microplate reader (Biotek, Northstar, Bedfordshire, UK).

**2.4. Scanning electron microscopy of bacteria challenged with PAMAM dendrimers**

*S. aureus* (ATCC 11832) and *E. coli* (ATCC 8277) were cultured, harvested and washed as described above except that an overnight culture of $10^8$ cells/mL was used to ensure that bacterial cells were at a sufficiently high density after the washes involved in preparation methods. 200 µL aliquots of a range of concentrations of each dendrimer (from 1-200 µg/mL for G2, G3 and G4-PAMAM-$NH_2$, and 0.0025-12.5 µg/mL for G5-PAMAM-$NH_2$) were constituted. For G3.5-PAMAM-COOH dendrimer the concentration range of solutions made were between 1-250 µg/mL. The PAMAM dendrimer solutions (200 µL) were added to 200 µL of the bacterial inoculum and incubated at 37°C ± 1°C for 2 hours and shaken at 200 rpm. After the incubation period the bacteria were centrifuged at 10,000 x *g* for 10 mins, resuspended in PBS (pH 7.4), centrifuged as above and the supernatant discarded. This was repeated 3 times to wash the harvested bacteria. The bacteria were then fixed in 2.5% glutaraldehyde in 0.1 M sodium cacodylate buffer (pH 7.4 containing 2 mM $CaCl_2$) for 2 hours on a low speed rotator.

Fixative was washed from the bacteria in sodium cacodylate buffer (pH 7.4 containing 2 mM $CaCl_2$) 3 times. A 100 µL aliquot of each fixed sample was added to a poly-*L*-lysine coated cover slip. The bacteria on the poly-*L*-lysine coated cover slips were then post-fixed in a solution of 1% sodium tetroxide in sodium cacodylate buffer. After a 1 hour contact time the osmium tetroxide was

removed by washing the cover slips in sodium cacodylate buffer (pH 7.4 containing 2 mM $CaCl_2$). The cover slips were then submerged in 70% ethanol and dehydrated at 4°C for 6 days. The samples were then further dehydrated for ten minutes each in 70%, 80%, 90% and 100% ethanol. To remove the solvent from the samples they were critical-point dried three times to replace the 100% ethanol with liquid $CO_2$ under pressure. Liquid $CO_2$ was subsequently removed by increasing the temperature (to 40°C) and pressure until the $CO_2$ vaporised. Samples were secured to a scanning electron microscope (SEM) stub mount, sputtered with gold and then placed in the high resolution (1.5 nm) field emission SEM (Hitachi, S4500).

**2.5. Statistical analysis of results**

Results are reported as the mean ± SEM (standard error of the mean) unless otherwise stated. All inner membrane permeabilisation data passed the D'Agostino and Pearson normality test ($\alpha = 0.05$) using GraphPad Prism® version 5 (San Diego, USA). For the inner membrane permeabilisation data a two-way ANOVA with a Bonferroni post-test was used to compare the two variables of dendrimer generation and dendrimer concentration at the various time points.

## 3. Results

### 3.1. Microdilution broth with viable count assay to determine the inhibitory concentration ($MIC_{50}$).

The inhibitory effect of PAMAM dendrimers against *S. aureus* and *E. coli* is shown in Table 1. For 50% inhibition of *S. aureus* the G2-PAMAM-$NH_2$ dendrimer required >9 times the concentration that was required for the G5-PAMAM-$NH_2$ dendrimer to exert the same effect. An increase in PAMAM generation from G2 to G5 showed that the $MIC_{50}$ (*S. aureus*) decreased substantially (Table 1). For the lowest concentrations of G2-PAMAM-$NH_2$ and G5-PAMAM-$NH_2$ tested, bacterial growth was observed when compared to the untreated growth control. The $MIC_{50}$ required to inhibit 50% of the *S. aureus* was approximately 2-fold higher than the concentration required to inhibit 50% of the *E. coli*. When challenged with *S. aureus* the carboxyl-terminated dendrimer resulted in minimal inhibition (Table 1). The $MIC_{50}$ against *S. aureus* decreased with increasing numbers of surface amine groups on the PAMAM dendrimer (Figure 1). An exponential inhibition curve was added to the graph which highlights the exponential increase in molecular weight and the number of amine surface groups with increasing PAMAM generation.

### 3.2. Membrane integrity study

Figure 2 indicates that, for all three bacterial strains, the absorbance at 260 nm increased with time with a plateau at 80 minutes (for *S. aureus*) and 100 minutes for both *S. epidermidis* and *E. coli*, respectively. The absorbance increase for *S. aureus* shows a linear trend to a plateau with data overlapping with the control up to 40 minutes , whereas with the absorbance for *S. epidermidis* increased monotonically up to a plateau at 100 minutes. *E. coli* showed an increase in absorbance over the first 60 minutes.

### 3.3. Inner membrane permeabilisation assay

In the inner membrane permeabilisation assay it was found that the absorbance reached a plateau at around 20 minutes. The mean absorbance at 420 nm for G2-PAMAM-$NH_2$, G3-PAMAM-$NH_2$, G4-PAMAM-$NH_2$, and G5-PAMAM-$NH_2$ was 0.222 (95% CI: 0.221-0.224) 0.228 (95% CI: 0.227-0.230), 0.228 (95% CI: 0.226-0.229) and 0.214 (95% CI: 0.213-0.216), respectively. A clear effect of concentration dependency on the inner membrane permeabilisation was observed when the vehicle control was compared to 5 µg/mL,when the concentrations 0.1 and 1.0 µg/mL of dendrimers were compared, there was no statistical difference ($p$>0.05). The inner membrane permeabilisation and thus production of *O*-nitrophenol, increased with increasing concentrations of the PAMAM dendrimer and with time (Figure 3). For all four PAMAM-$NH_2$ dendrimer generations tested, a concentration as low as 5 µg/mL resulted in permeabilisation of the inner membrane by 12 minutes (Figure 3). The production of *O*-nitrophenol varied across the four PAMAM generations tested. The highest concentration tested (50 µg/mL) demonstrated the greatest increase in absorbance, therefore inducing the highest degree of inner membrane permeabilisation. However, the exception to this was the G5-PAMAM-$NH_2$ dendrimer. At a particular time point of 4-10 minutes, 25 µg/mL solution of G5-PAMAM-$NH_2$ dendrimer showed a higher absorbance at 420 nm and thus *O*-nitrophenol production than at a 50 µg/mL concentration. G5-PAMAM-$NH_2$ dendrimer also demonstrated a longer lag period for absorbance increase at 420 nm due to its high molecular weight and diameter causing slow passive diffusion across the cell wall and membrane. At a concentration of 5 µg/mL and based on the mean across all time points for a specific concentration, the order from the highest absorbance and thus production of o-nitrophenol to the lowest was G2>G3>G5>G4. At a higher dendrimer concentration of 50 µg/mL the absorbance measurement trend in decreasing order was G3>G4>G2>G5.

A final measurement of *O*-nitrophenol production was taken at 60 minutes (Figure 4). It was established that even after 60 minutes no change in absorbance was observed for concentrations below 5 µg/mL ($p$>0.05). With the exception of 0.1 and 1 µg/mL of PAMAM dendrimer, there was a

significant difference in absorbance when comparing all concentrations of each PAMAM generation to the vehicle control ($p$<0.001).. A generation effect was also observed, to a degree, when comparing the absorbance at 420 nm of various PAMAM dendrimer generations over 12 minutes at 50 µg/mL (Figure 5).

**3.4. Scanning electron microscopy of bacteria challenged with PAMAM dendrimers**

Figure 6 (a-b) shows an electron micrograph of *S. aureus* bacteria. When compared to the G3-PAMAM-NH2 at a concentration of 5 times the $MIC_{50}$ (µg/mL), varying degrees of membrane damage was observed from minor blebbing through to total destruction of the cell membrane and cell wall (Figure 6 (c-d)). This was also found to be the case with G2-PAMAM-NH2 (Figure 6 (e-f)) and G5-PAMAM-NH2 (Figure 6 (g-h)). The SEM images demonstrate the ability for G2-PAMAM-NH2 and G5-PAMAM-NH2 to cause severe bacterial cell membrane and cell wall damage, including blebbing of cytoplasmic contents from damaged cell , and in some cases complete cell lysis. Sheets of bacterial cell wall and cytoplasmic content debris can be observed in the PAMAM treated bacteria images (Figure 6 (a-h)). For G3.5-PAMAM-COOH at a concentration of 1 mg/mL (Figure 6 (i-j)) there was no difference in bacterial cell morphology or changes to the integrity of the bacterial cell membrane or cell wall when compared to the untreated *S. aureus* group.

SEM images were also collected for the Gram-negative, rod-shaped *E. coli* bacteria. Figure 7 (a-b) shows the intact PAMAM untreated group micrographs. Figure 7(c-d) illustrates the G3-PAMAM-$NH_2$ treated group. Damage to the bacterial wall and cell membranes can be observed due to leakage of the cytoplasmic contents from the cell and blebbing. The PAMAM dendrimer typically targeted the polar regions of the *E. coli* rods, consistent to the findings observed by others[35]. Again, no changes in cell morphology were observed for the G3.5-PAMAM-COOH at a concentration of 1 mg/mL.

**4. Discussion**

A clear, generation-dependent trend was observed when the $MIC_{50}$ of each PAMAM generation was related to their respective theoretical number of surface amine groups. There was an inverse correlation between the $MIC_{50}$ concentration and PAMAM dendrimer generation. It was found that by increasing the number of amine groups on the dendrimer surface the concentration required to inhibit 50% of the bacteria dramatically decreased. Enhanced destabilization of bacterial membranes has been observed by increasing the number of amino groups on a polycation[17]. This generation-dependent trend was contrary to the findings elsewhere[15] where it was observed that the MIC for G3-PAMAM-$NH_2$ and G5-PAMAM-$NH_2$ against *S. aureus* was identical. A distinction in MIC value was found for two different PAMAM generations against *P. aeruginosa* as G3-PAMAM-$NH_2$ and G5-PAMAM-$NH_2$ exhibited a MIC of 6.3 µg/mL and 12.5 µg/mL, respectively. The authors suggest the difference is due to the G3-PAMAM-$NH_2$ dendrimer's ability to penetrate the cell more easily due to its lower molecular weight compared to G5-PAMAM-$NH_2$. This effect was not observed in the present study, possibly due to differences in the chemical nature of the G3 and G5 dendrimers used in our study and the study by Lopez et al., respectively[15].

Another apparent trend is that PAMAM dendrimers are more effective against Gram-negative bacteria such as *E. coli*., a finding echoed elsewhere[14]. *E. coli* has a very different cell wall structure and composition compared to the Gram positive *S. aureus*. The outer membrane of *E. coli.* consists of lipopolysaccharide (LPS), phospholipids and proteins[18]. LPS carries a high anionic charge at physiological pH due to the ionisable phosphoryl and carboxyl groups[19]. The polycationic nature of PAMAM dendrimers ensures high reactivity with, and affinity for, the outer membrane due to strong electrostatic forces. The high degree of interaction and disruption of the lipid bilayer of the outer membrane with the polycationic PAMAM dendrimer, reported previously[14], is one possible

explanation for the enhanced antimicrobial efficacy observed for Gram-negative bacteria and for G5-PAMAM-$NH_2$ tested against *P. aeruginosa*.

The results indicate that G3- PAMAM-$NH_2$ causes intracellular components to leak from *S. aureus*, *S. epidermidis* and *E. coli* within approximately 20 minutes. Precipitation and coagulation of nucleotides has been observed for other cations[20] and has potentially occurred with the concentration of PAMAM dendrimer. . The inner membrane consists of a complex proteome within a lipid bilayer. This is formed principally from phosphatidyl ethanolamine, phosphatidyl glycerol, and to a lesser extent cardiolipin, the latter two of which carry anionic charges[21]. Our results indicate that the polycationic PAMAM dendrimers have a strong affinity for the anionic inner membrane of *E. coli*. These novel results suggest that there are important time, concentration- and dendrimer generation-dependent effects on the inner membrane permeabilisation of *E. coli.*

Structural and morphological changes induced by the dendrimers are shown in Figures 6 and 7. The *S. aureus* samples showed blebbing of cytoplasmic material on the cell surface that had been presumably extruded from a damaged cell membrane. Leaked cytoplasmic material, severe membrane damage and even separation of the cell membrane of the bacteria from the cell was also observed, caused by the different generations of PAMAM dendrimers. The degree of cell damage observed is consistent with previous studies of the cationic biocides polyquaternium-1 and myristamidopropyl dimethylamine[22]. Further, comparable cytoplasmic membrane damage was observed for *S. aureus* when challenged with the essential oil isolated from *O. Vulgare*[23]. Marked release of cytoplasmic contents was also observed for *E. coli* due to membrane damage inflicted by the G3-PAMAM-$NH_2$ dendrimer, which is again consistent with previous findings with tea tree oil[24], and, in one case, with the G4-PAMAM-$NH_2$ dendrimer[25], which resulted in rupturing of cell walls,

erosion of cell membranes and shrinkage of bacterial cells. Thus the SEM images herein suggest that the mechanism of action of PAMAM dendrimers is to target and disrupt the bacterial cell membrane.

**5. Conclusions**

This study has confirmed that the antimicrobial efficacy of native PAMAM dendrimers is dependent on generation, concentration and terminal functionalities. There was a strong correlation between membrane disruption and the determined biocidal activity, thus making it a key contributor to the mechanism of action. This study has shown that selection of the type of PAMAM dendrimer is important as their inherent antimicrobial efficacy is dependent on the physicochemical properties of specific dendrimers. Such correlations between structure and biocide function will allow a more appropriate and focused use of dendrimers in this role. Recently, for example, it was reported that following the pre-treatment of skin with a G3-PAMAM dendrimer, the subsequent skin permeation of chlorhexidine was significantly enhanced. This clearly indicates that the strategy for increasing antimicrobial efficacy with dendrimers is viable, either as a single treatment or in combination with other treatments[26]. G5-PAMAM-$NH_2$ dendrimer would also be the most suitable polymer for biocidal applications as it shows the greatest efficacy against both Gram negative and Gram positive bacteria. Thus, this study clearly demonstrates the antimicrobial potential of dendrimers and that optimising their efficacy is based on dendrimer physicochemical properties. Through this understanding an informed choice may be made as to which PAMAM dendrimer to select as part of a quality-by-design approach to developing novel biocides.

**Declarations**

**Funding**

This work was funded by an EPSRC CASE award (R4504 A779) in collaboration with Dermal Technology Laboratory Ltd.

**Competing Interests:** The authors have no conflicts of interest to disclose.

**Ethical Approval:** Not required

**Acknowledgements**

The authors would like to acknowledge and thank Professor Stephen Chapman (School of Pharmacy, Keele University, UK) for his assistance with this study.

**References**


1. Davis KA, Stewart JJ, Crouch HK, Florez CE, Hospenthal DR. Methicillin-resistant Staphylococcus aureus (MRSA) nares colonization at hospital admission and its effect on subsequent MRSA infection. Clin. Infect. Disease 2004; 39:776-82.
2. Von Eiff C, Becker K, Machka K, Stammer H, Peters G. Nasal carriage as a source of Staphylococcus aureus bacteremia. New Eng. J. Med 2001; 344:11-6.
3. McCarthy TD, Karellas P, Henderson SA, Giannis M, O'Keefe DF, Heery G, Paull JRA, Matthews BR, Holan G. Dendrimers as drugs: discovery and preclinical and clinical development of dendrimer-based microbicides for HIV and STI prevention. Mol. Pharmacol. 2005;2:312-8.
4. Mammen M, Choi SK, Whitesides GM. Polyvalent interactions in biological systems: implications for design and use of multivalent ligands and inhibitors. Angewandte Chemie Int. Edn. 1998;37:2754-94.
5. Morones JR, Elechiguerra, JL, Camacho, A, Holt K, Kouri JB, Ramirez JT, Yacaman MJ. The bactericidal effect of silver nanoparticles. Nanotech. 2005;16:2346-53.
6. Balogh L, Swanson DR, Tomalia DA, Hagnauer GL, McManus AT. Dendrimer-silver complexes and nanocomposites as antimicrobial agents. Nano Let. 2001;1:18-21.
7. Svenson S. Dendrimers as versatile platform in drug delivery applications. Eur. J. Pharm. Biopharm. 2009; 71:445-62.
8. Esfand R, Tomalia DA. Poly (amidoamine)(PAMAM) dendrimers: from biomimicry to drug delivery and biomedical applications. Drug Discov. Today 2001;6:427-36.
9. Sajja HK, East MP, Mao H, Wang AY, Nie S, Yang L. Development of Multifunctional Nanoparticles for Targeted Drug Delivery and Non-invasive Imaging of Therapeutic Effect. Curr. Drug Discov. Technol. 2009; 6:43-51.
10. Meyers SR, Juhn FS, Griset AP, Luman NR Grinstaff MW. Anionic amphiphilic dendrimers as antibacterial agents. J. Am. Chem. Soc. 2008; 130:1444-5.
11. Zhang L, Pornpattananagkul D, Hu C, Huang C. Development of Nanoparticles for Antimicrobial Drug Delivery. Curr. Med. Chem. 2010; 17:585-94.

12. Tomalia DA, Naylor AM, Goddard WA. Starburst dendrimers: molecular-level control of size, shape, surface chemistry, topology, and flexibility from atoms to macroscopic matter. Angewandte Chemie Int. Edn. 1990;29:138-75.
13. Gillies ER, Frechet JMJ. Dendrimers and dendritic polymers in drug delivery. Drug Discov. Today 2005;10:35-43.
14. Calabretta MK, Kumar A, McDermott AM, Cai C. Antibacterial activities of poly (amidoamine) dendrimers terminated with amino and poly (ethylene glycol) groups. Biomacromol. 2007;8:1807-11.
15. Lopez AI, Reins RY, McDermott AM, Trautner BW, Cai C. Antibacterial activity and cytotoxicity of PEGylated poly (amidoamine) dendrimers. Mol. Biosystems. 2009;5:1148-56.
16. Rennie R. NCCLS: Evaluation of Lots of Dehydrated Mueller-Hinton Broth for Antimicrobial Susceptibility Testing; Proposed Guideline. NCCLS document M32-P [ISBN 1-56238-447-3]. NCCLS, 940 West Valley Road, Suite 1400, Wayne, Pennsylvania 19087-1898 USA, 2001.
17. Katsu T, Nakagawa H, Yasuda K. Interaction between polyamines and bacterial outer membranes as investigated with ion-selective electrodes. Antimicrob. Agent. Chemotherap. 2002;46:1073-9.
18. Nikaido H. Multidrug efflux pumps of gram-negative bacteria. J. Bacteriolog. 1996;178:5853-9.
19. Beveridge TJ. Structures of gram-negative cell walls and their derived membrane vesicles. J. Bacteriolog. 999;181:4725-33.
20. Hugo W, Longworth A. Effect of chlorhexidine diacetate on “protoplasts” and spheroplasts of *Escherichia coli,* protoplasts of *Bacillus megaterium* and the gram staining reaction of *Staphylococcus aureus*. J. Pharm Pharmacol. 1964;16:751-758.
21. Dowhan W. Molecular basis for membrane phospholipid diversity: why are there so many lipids? Ann. Rev. Biochem. 1997;66:199-232.
22. Codling CE, Hann AC, Maillard JY, Russell A. An investigation into the antimicrobial mechanisms of action of two contact lens biocides using electron microscopy. Contact Lens and Anterior Eye, 2005;24:163-8.
23. De Souza EL, Barros JC, De Oliveira CEV, Da Conceicao ML. Influence of *Origanum vulgare* L. essential oil on enterotoxin production, membrane permeability and surface characteristics of *Staphylococcus aureus*. Int. J. Food Micro. 2010;137:308-311.

24. Gustafson J, Liew Y, Chew S, Markham J, Bell H, Wyllie S, Warmington J. Effects of tea tree oil on *Escherichia coli*. Let. App. Micro. 1998;26: 194-8.

25. Wang B, Navath RS, Menjoge AR, Balakrishnan B, Bellair R, Dai H, Romero R, Kannan S, Kannan RS. Inhibition of bacterial growth and intramniotic infection in a guinea pig model of chorioamnionitis using PAMAM dendrimers. Int. J. Pharm. 2010;395:298-308.

26. Holmes AM, Scurr DJ, Heylings JR, Wan KW, Moss GP. Dendrimer pre-treatment enhances the skin permeation of chlorhexidine digluconate: Characterisation by in vitro percutaneous absorption studies and Time-of-Flight Secondary Ion Mass Spectrometry. Eur. J. Pharm. Sci. 2017;104:90-101.

27. Chen, C.Z. and Cooper, S.L., Interactions between dendrimer biocides and bacterial membranes. Biomat. 2002;**23**(16):3359-3368.

28. Je, J.Y. and Kim, S.K.,Chitosan derivatives killed bacteria by disrupting the outer and inner membrane. *Journal of Agricultural and Food Chemistry,* 2006;**54**(18):6629-6633.

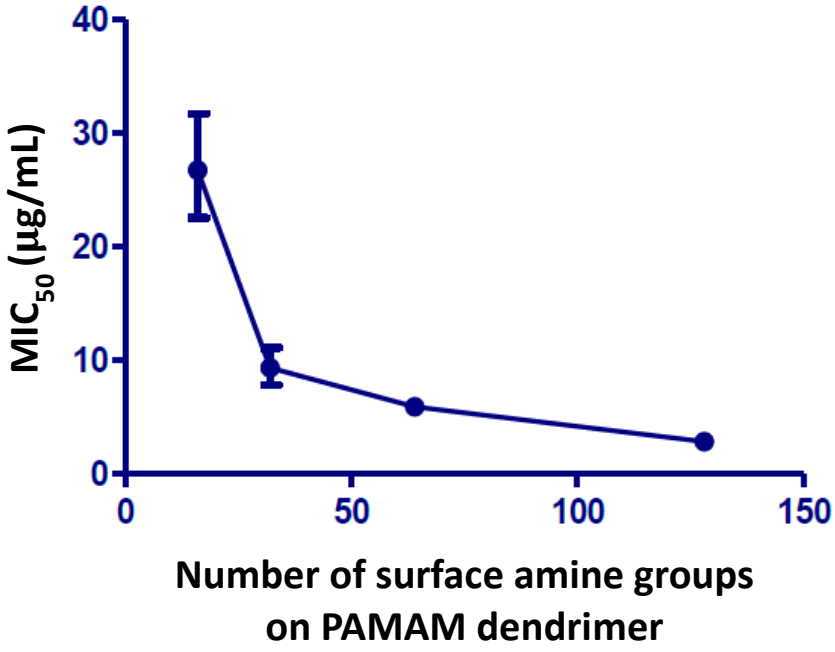


Figure 1. Graph illustrating the calculated $MIC_{50}$ (µg/mL) concentrations. $MIC_{50}$ (µg/mL) with error bars representing 95% confidence intervals (n=3) against *S. aureus* plotted against the theoretical number of surface amine groups corresponding to G2-PAMAM-$NH_2$, G3-PAMAM-$NH_2$, G4-PAMAM-$NH_2$ and G5-PAMAM-$NH_2$ dendrimers.

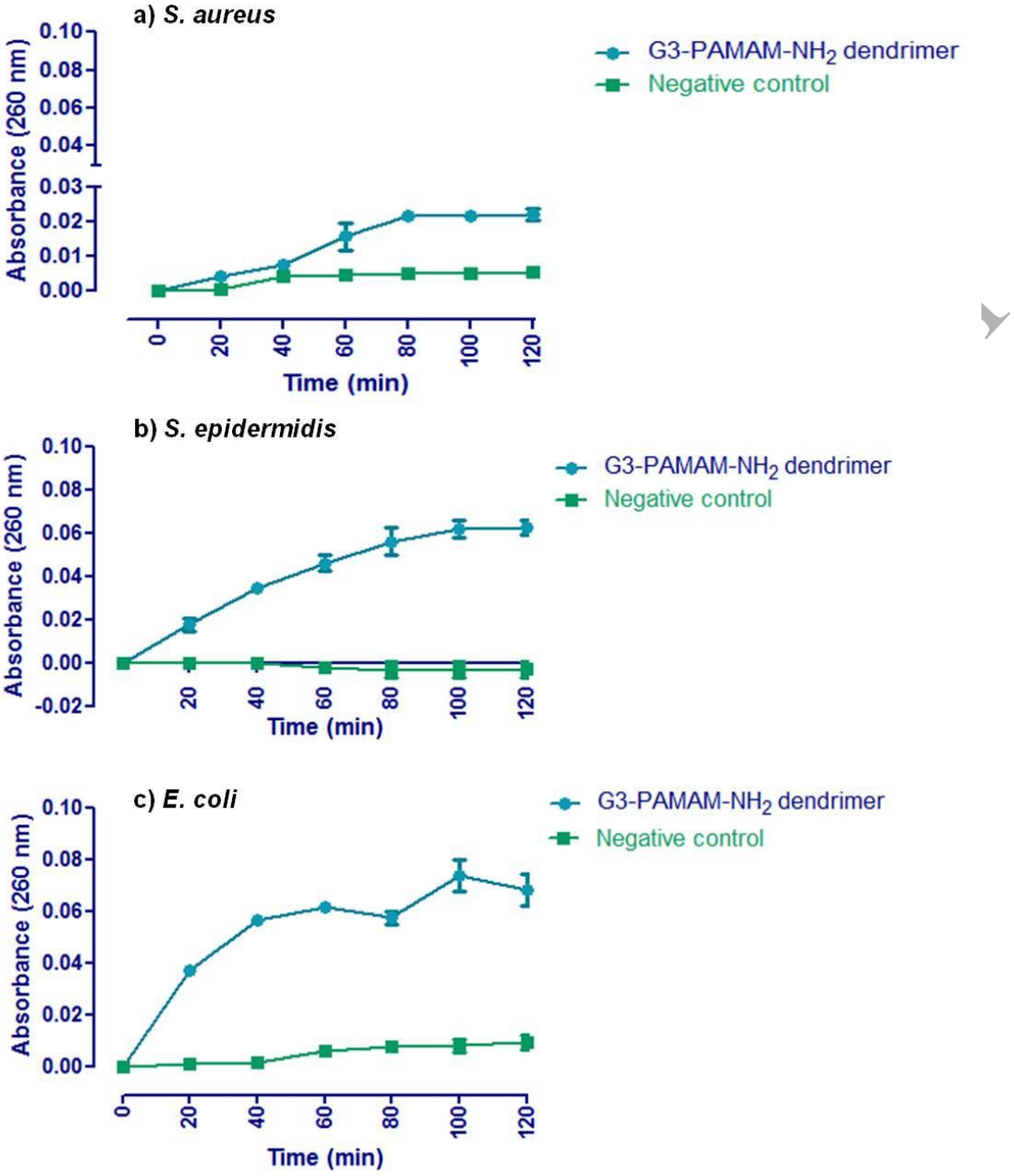


Figure 2 Graphs illustrating the release of nuclear material from *S. aureus*, *S. epidermidis* and *E. Coli:* (a) Absorbance at 260 nm plotted against time for *S. aureus* challenged against G=3 x 5 $MIC_{50}$; (b) Absorbance at 260 nm plotted against time for *S. epidermidis* challenged against G=3 x 5 $MIC_{50}$; (c) Absorbance at 260 nm plotted against time for *E. coli* challenged against G=3 x 5 $MIC_{50}$. All results are displayed as (n=3) mean ± standard deviation. Negative control was the absorbance at 260 nm for the untreated bacteria group.

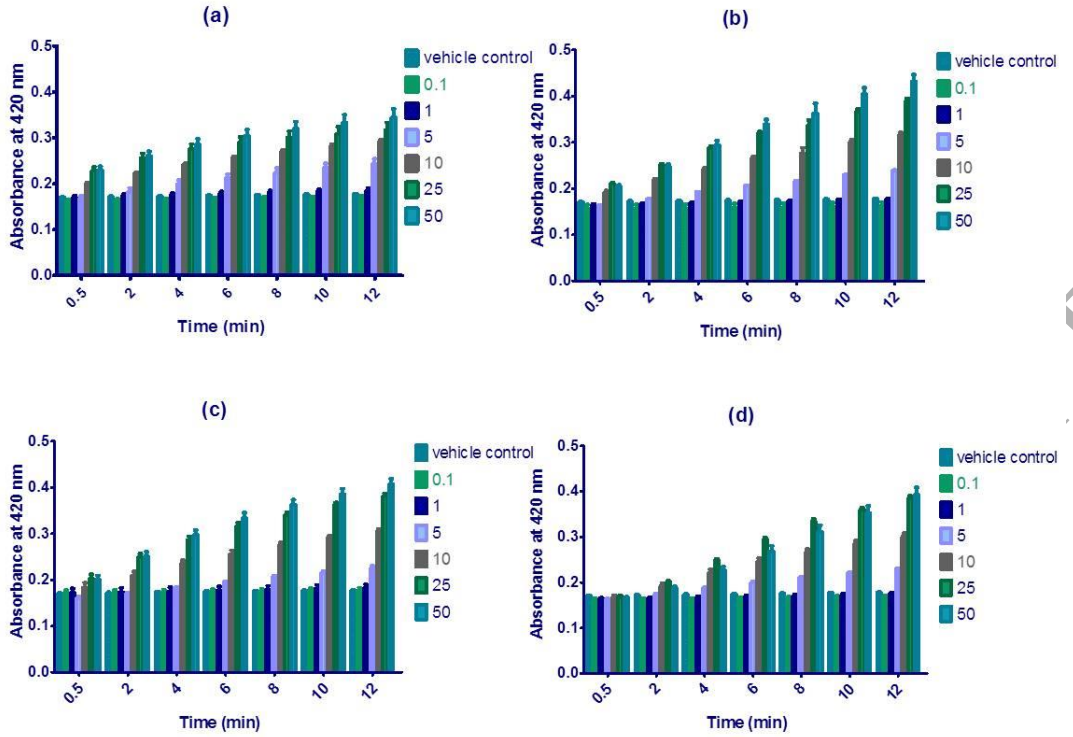


Figure 3. Graphs illustrating the relationship between concentration, time and dendrimer generation on the inner membrane permeabilisation of *E. coli*; (a) corresponds to G2-PAMAM-$NH_2$ treated *E. coli*; (b) G3-PAMAM-$NH_2$ treated *E. coli*; (c) G4-PAMAM-$NH_2$ treated *E. coli* and (d) G5- PAMAM-$NH_2$ treated *E. coli*. Vehicle control is displayed as the untreated control group. All results shown represent the mean ± SEM (n=3)

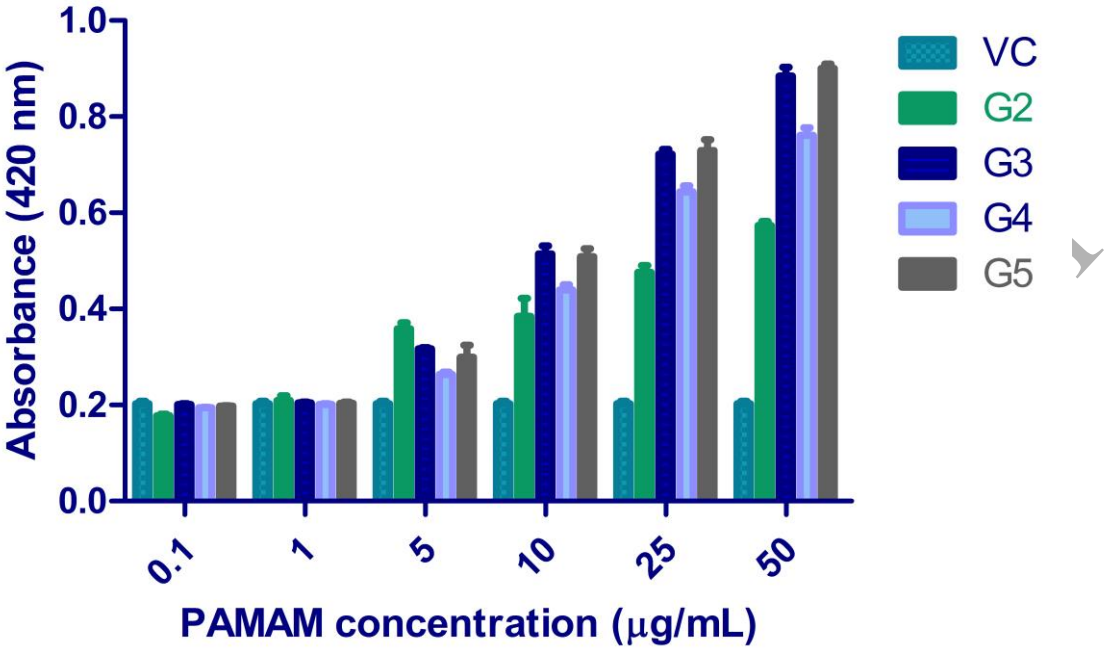


Figure 4. Graph illustrating the inner membrane permeabilisation of *E.* coli at 60 minutes for a range of dendrimer concentrations. Absorbance at 420 nm plotted against a range of dendrimer concentrations (0.1- 50 µg/mL) at 60 minutes. G2 corresponds to G2-PAMAM-$NH_2$ treated *E. coli*, G3 G3-PAMAM-$NH_2$ treated E. coli, G4-PAMAM-$NH_2$ treated E. coli and (c) G5-PAMAM-$NH_2$ treated *E. coli*. VC corresponds to the vehicle control and is displayed as the untreated bacteria group control. All results shown represent the mean ± SEM (n=3). All PAMAM treated samples are significantly different ($P<0.001$) from the vehicle control for the concentration range 5-50 µg/mL.

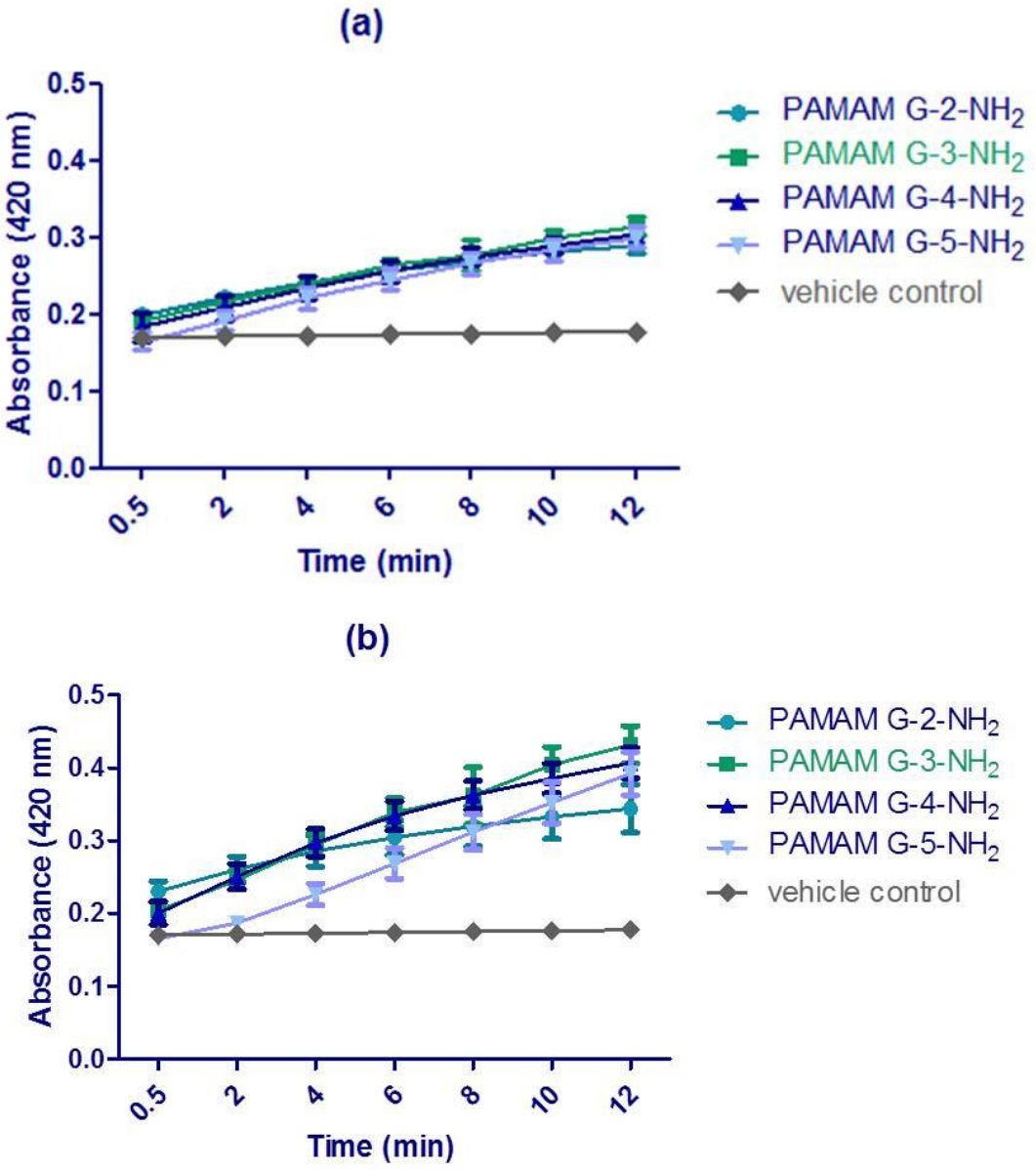


Figure 5. Graphs illustrating the effect of dendrimer generation and time at specific concentrations on the inner membrane permeabilisation of *E. coli.* Absorbance at 420 nm plotted against time in minutes, (a) corresponds to each PAMAM generation at a concentration of 10 µg/mL challenged against *E. coli* and (b) PAMAM generations at a concentration of 50 µg/mL challenged against *E. coli.* VC corresponds to the vehicle control and was displayed as the untreated bacteria group control. All results shown represent the mean ± SEM (n=3). All treated sample values are significantly different ($P<0.05$)from the vehicle control with the exception of the 0.5 min time points and 2 minutes for G5 PAMAM at both concentrations tested.

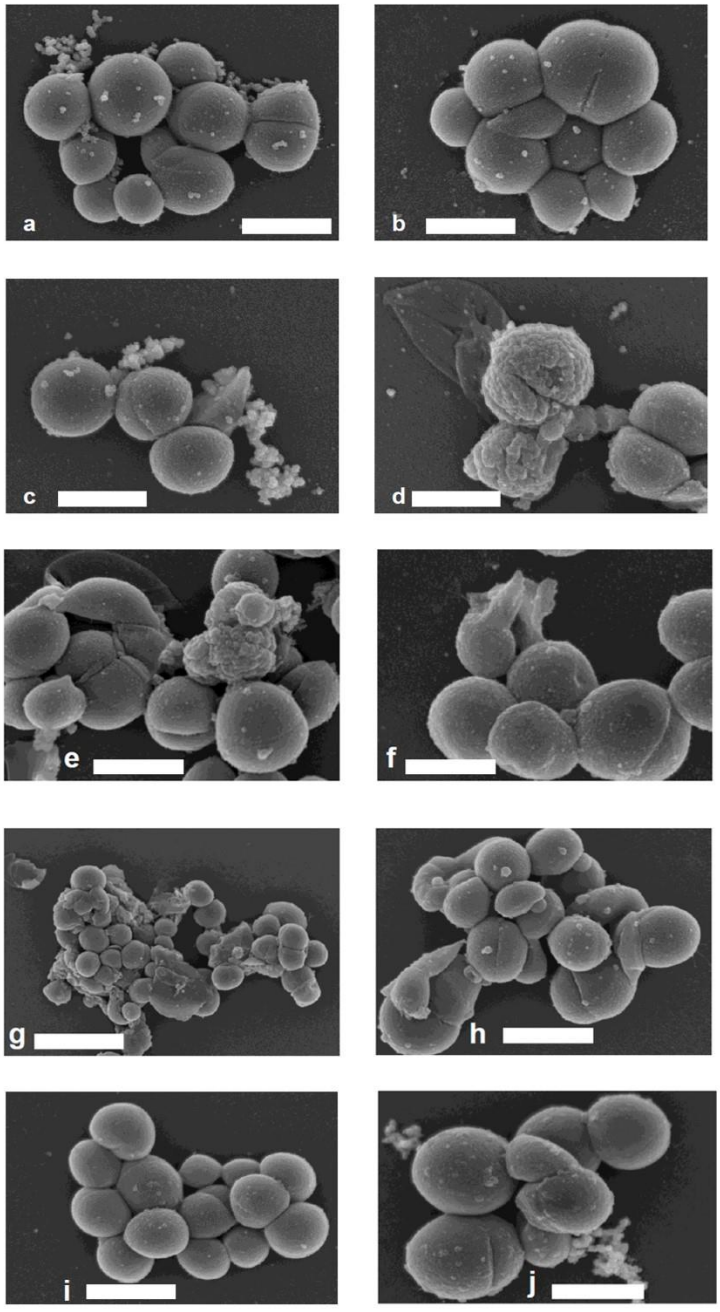


Figure 6. Scanning electron micrographs of *S. aureus* challenged with PAMAM dendrimer. (a) untreated *S. aureus* at a magnification of x 25k, scale bar represents 1 µm. (b) untreated *S. aureus* at a magnification of x 30k, scale bar represents 1 µm. (c) *S. aureus* treated with G3-PAMAM-$NH_2$ at a concentration of 5 x calculated $IC_{50}$. Magnification x 30k and scale bar represents 1 µm. (d) S. aureus treated with G3-PAMAM-$NH_2$ at a concentration of 5 x calculated $IC_{50}$. Magnification x 30k and scale bar represents 1 µm. (e) *S. aureus* treated with G2-PAMAM-$NH_2$ at a concentration of 250 µg/mL, magnification x 25k and scale bar represents 1 µm. (f) *S. aureus* treated with G2-PAMAM-$NH_2$ at a concentration of 250 µg/mL, magnification x 40 k and scale bar represents 1 µm. (g) *S. aureus* treated with G5-PAMAM-$NH_2$ at a concentration of 250 µg/mL, magnification x10k and scale bar represents 3 µm. (h) *S. aureus* treated with G5-PAMAM-$NH_2$ at a concentration of 250 µg/mL, magnification x20k and scale bar represents 1 µm. (i) S. aureus treated with G3.5-PAMAM-COOH at a concentration of 1000 µg/mL, magnification x25k and scale bar represents 1 µm. (j) *S. aureus* treated with G3.5-PAMAM-COOH at a concentration of 1000 µg/mL, magnification x30k and scale bar represents 1 µm.

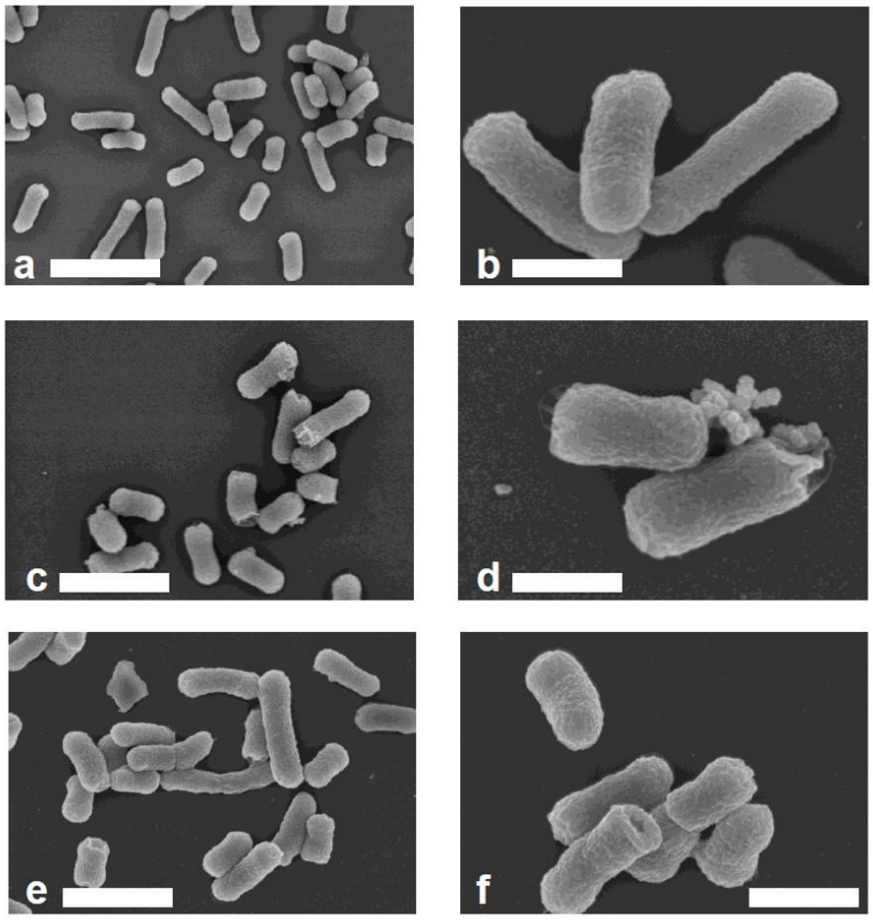


Figure 7. Scanning electron micrographs of *E. coli* challenged with PAMAM dendrimer. (a) *E. coli* untreated magnification x 10 k scale bar scale bar represents 2 μm. (b) *E. coli* untreated magnification x 40 k scale bar scale bar represents 1.5 μm. (c) *E. coli* treated G3-PAMAM-$NH_2$ at a concentration of 5 x calculated $IC_{50}$, magnification x 15 k and scale bar represents 2 μm. (d) *E. coli* treated G3-PAMAM-$NH_2$ at a concentration of 5 x calculated $IC_{50}$, magnification x 50 k and scale bar represents 1.5 μm. (e) *E. coli* treated with 1000 μg/mL of G3.5-PAMAM-COOH magnification x 15 k scale bar 2 μm. (f) *E. coli* treated with 1000 μg/mL of G3.5-PAMAM-COOH magnification x 30 k scale bar 1.5 μm.

Table 1. Dendrimer physicochemical characteristics and calculated $MIC_{50}$ (μg/mL) with 95% confidence intervals against *S. aureus* and *E. coli*.

| Bacteria | PAMAM generation | Molecular Weight (g/moL) | No. of amine surface groups | $MIC_{50}$ (95% CI) μg/mL |
|---|---|---|---|---|
| *Staphylococcus aureus* | G2-PAMAM-$NH_2$ | 3,256 | 16 | 26.77 (22.58- 31.75) |
| | G3-PAMAM-$NH_2$ | 6,909 | 32 | 9.374 (7.88- 11.15) |
| | G4-PAMAM-$NH_2$ | 14,215 | 64 | 5.962 (5.375- 6.614) |
| | G5-PAMAM-$NH_2$ | 28,826 | 128 | 2.881 (2.473- 3.355) |
| | G3.5-PAMAM-COOH | 12,927 | 64 | > 250 |
| *Escherichia coli* | G3-PAMAM-$NH_2$ | 6,909 | 32 | 4.931 (4.28- 5.679) |
| | G3.5-PAMAM-COOH | 12,927 | 64 | >1000 |